J Mater Sci: Mater Med (2010) 21:1479–1488
DOI 10.1007/s10856-010-3990-z

Surface modification of a Ti–7.5Mo alloy using NaOH treatment and Bioglass® coating

Wen-Fu Ho · Chien-Hung Lai · Hsueh-Chuan Hsu ·
Shih-Ching Wu

Received: 31 March 2009 / Accepted: 4 January 2010 / Published online: 13 January 2010

Abstract The objective of this study was to propose a surface modification for a low-modulus Ti–7.5Mo alloy to initiate the formation of hydroxyapatite (HA) during in vitro bioactivity tests in simulated body fluid (SBF). Specimens of commercially pure titanium (c.p. Ti) and Ti–7.5Mo were initially immersed in a 15 M NaOH solution at 60°C for 24 h, resulting in the formation of a porous network structure composed of sodium titanate ($Na_2Ti_5O_{11}$). Afterwards, bioactive Bioglass® particles were deposited on the surface of NaOH-treated c.p. Ti and Ti–7.5Mo. The specimens were then immersed in SBF at 37°C for 1, 7 and 28 days, respectively. The apatite-forming ability of the NaOH-treated and Bioglass®-coated Ti–7.5Mo was higher than that of the c.p. Ti under the same condition. The X-ray diffraction (XRD) and energy-dispersive X-ray spectroscopy (EDS) results indicated that the deposited amounts of calcium phosphate were much greater for the surface-treated Ti–7.5Mo than for the c.p. Ti, a finding attributable to or correlated with the higher pH value of the SBF containing surface-treated Ti–7.5Mo. Moreover, in the surface-treated Ti–7.5Mo, the pH value of the SBF approached a peak of 7.66 on the first day. A combination of NaOH treatment and subsequent Bioglass® coating was successfully used to initiate in vitro HA formation in the surface of the Ti–7.5Mo alloy.

1 Introduction

Titanium and its alloys are widely used for load-bearing dental and orthopedic implants because of their superior mechanical properties, good biocompatibility and high corrosion resistance. However, titanium alloys do not bond directly to living bone [1, 2], a situation which can lead to encapsulation by dense fibrous tissue in the body [3, 4]. Consequently, inappropriate stress distribution at the bone-implant interface appears, which could lead to interfacial failure and loosening of the implants. It is well recognized that calcium phosphate coatings have led to better long-term clinical success rates than uncoated titanium implants [5, 6]. Various methods have been developed for coating metal implants: plasma-spraying, sputter-deposition, sol–gel coating, electrophoretic deposition or biomimetic deposition [7–14]. A plasma-sprayed hydroxyapatite (HA) coating has been most successfully and widely applied [13], reportedly showing beneficial effects such as osteoconductivity and direct-bone bonding ability [13]. However, this method has disadvantages attributed to the high temperatures used during the process, such as the possibility of fracture at the interface between the titanium and the HA due to the residual stress at the interface and changes in the composition, porosity, crystallinity and structure of the plasma-sprayed HA [15]. Furthermore, in the case of HA coatings prepared by electrodeposition,

W.-F. Ho (✉)
Department of Materials Science and Engineering, Da-Yeh University, 168 University Road, Dacun, Changhua 51591, Taiwan, ROC
e-mail: fujii@mail.dyu.edu.tw

C.-H. Lai
Department of Mechanical and Automation Engineering, Da-Yeh University, Changhua, Taiwan, ROC

H.-C. Hsu · S.-C. Wu
Department of Dental Laboratory Technology, Central Taiwan University of Science and Technology, Taichung, Taiwan, ROC

H.-C. Hsu · S.-C. Wu
Institute of Biomedical Engineering and Material Science, Central Taiwan University of Science and Technology, Taichung, Taiwan, ROC

their bonding with the titanium implant has been found unsatisfactory [16].

Several researchers have proposed various chemical treatments, including NaOH [17, 18] or H_2O_2 solutions [19, 20] to provide osteoconductivity to titanium. These treatments create Ti–OH groups in a titania hydrogel layer on the titanium surface. It has also been reported that Ti–OH provides a catalytic effect to trigger heterogeneous nucleation of HA in a simulated body fluid (SBF) [21, 22]. Biomimetic deposition of HA has attracted widespread interest because of its low deposition temperature and good step coverage. Moreover, some studies have achieved a higher bone-to-implant contact for biomimetic calcium phosphate coatings than for uncoated titanium implants [7, 23].

Recently, Bil et al. [24] proposed that polyurethane (PUR) and polyurethane/poly(D, L-lactide) acid (PUR/PDLLA) based scaffolds coated with Bioglass® particles for application in bone tissue engineering were fabricated by a slurry-dipping method. The homogeneous structure of the Bioglass® coatings on the surface of the PUR and PUR/PDLLA foams indicated a good adhesion of the bioactive glass particles to polyurethane without any additional surface treatment. Moreover, bioactive and bioresorbable polymers have also been developed based on three-dimensional, macroporous PDLLA foams and Bioglass® particles. The slurry-dipping technique led to stable and uniform glass coatings as well as adequate infiltration of Bioglass® into the porous network of the foams [25]. The slurry-dipping in distilled water gave the best results in terms of production of uniform and reproducible bioactive glass coatings, and provided a better bioactive behavior of the coated sutures in terms of kinetics of HA precipitation and quality of the precipitated layers [26].

In the past few years, new Ti alloys have been extensively investigated and developed for biomedical applications as possible substitutes for the well-established Ti–6Al–4V alloy [27–29]. Although this alloy exhibits excellent mechanical and corrosion properties, it contains vanadium, which is known to be cytotoxic [30]. Thus, avoiding metal ion release and obtaining vanadium-free alloys has been the focus of recent investigations [31–33]. Another important requirement for implants designed to replace or interact with bone is low elastic modulus matching, as closely as possible, to that of the surrounding bone tissue [34]. Ti–7.5Mo is a new α''-phase alloy possessing a lower elastic modulus, an improved strength/modulus combination [35] and excellent corrosion resistance [36]. However, similar to other biomedical titanium alloys, it remains a bioinert material.

The classical biomimetic calcium phosphate coatings normally require an immersion period of about 14–28 days with replenishment from an SBF solution. Very recently, efforts have been made [37–40] to accelerate this process to increase its practical utility. In the present study, attempts were made to develop a biomimetic calcium phosphate coating on low-modulus Ti–7.5Mo alloy substrates treated with NaOH aqueous solutions and bioactive glass coatings by immersing them into SBF. The results were compared with commercially pure titanium (c.p. Ti) chosen as a control. Moreover, high-heat treatments were carefully avoided because the metastable α''-phase Ti–7.5Mo alloy is very sensitive to temperature. Furthermore, a high-temperature treatment process tends to result in the crystallization of the hydrogel layer, thereby reducing the ionic activity and decreasing the rate of apatite nucleation and formation [41]. Previous studies have revealed that the essential prerequisite for artificial materials to show osteoconductivity is the formation of a bone-like apatite layer on their surfaces after implantation in bony defects [42–44]. This alloy could become an attractive biomaterial, especially if made bioactive.

2 Experimental procedures

The materials used for this study included c.p. Ti and a Ti–7.5Mo alloy. (Note: All compositions are expressed by mass.) All the materials were prepared from raw titanium (99.8% pure) and molybdenum (99.95% pure) by using a commercial arc-melting vacuum-pressure-type casting system (Castmatic, Iwatani Corp., Japan). The ingots of approximately 30 g each were re-melted three times, at about 55 s each, to improve their chemical homogeneity. Prior to casting, the ingots were again re-melted. The difference in pressure between the two chambers allowed the molten alloys to instantly drop into a graphite mold at room temperature.

In this study, the cast alloys were sectioned by using a Buehler Isomet low-speed diamond saw to obtain specimens. Flat sheets of c.p. Ti and of Ti–7.5Mo, $1 \times 10 \times 10$ mm^3 each, were used as substrate materials. The surfaces of the metals were abraded to the final level of 2000-grit paper. The metal substrates were then ultrasonically cleaned in distilled water, acetone and ethanol for 20 min, respectively, after which the substrate plates were again cleaned in distilled water for another 10 min. Subsequently, the cleaned specimens were immersed in 15 M NaOH aqueous solutions at 60°C for 24 h. The temperature was maintained by using a water bath. After the 24 h incubation period, the substrates were gently washed with distilled water and dried at 40°C for 24 h.

In this research, 45S5 Bioglass® particles were used wherein the bioactive glass (45.0 SiO_2, 24.5 CaO, 24.5 Na_2O, and 6.0 P_2O_5 in wt%) was obtained from high-purity SiO_2, Na_2CO_3, $CaCO_3$ and P_2O_5 powders. To manufacture

Table 1 Ionic concentrations (mM) of simulated body fluid compared to human blood plasma [45]

	Na^+	K^+	Mg^{2+}	Ca^{2+}	Cl^-	HPO_4^{2-}	SO_4^{2-}	HCO_3^-
SBF	142.0	5.0	1.5	2.5	148.8	1.0	0.5	4.2
Blood plasma	142.0	5.0	1.5	2.5	103.8	1.0	0.5	27.0

the bioactive glass coatings, a slurry with glass powder (particle size <20 μm) in ethanol was poured into a beaker where subsequently alkali-treated specimens were put. The suspension of particles was dispersed by using a magnetic stirrer to achieve a uniform deposition on the specimen surface. After 24 h of dwelling time, the specimens were removed and placed in an oven at 40°C for 24 h to completely dry the green-coatings. After the NaOH treatment and bioactive glass coatings, the surfaces of the specimens were examined by scanning electron microscopy (SEM; JSM-6700F, JEOL, Japan) and X-ray diffractometry (XRD; D8 SSS, Bruker, Germany).

To test the capability of the material to spontaneously form a bonelike apatite layer in vitro, the glass-coated c.p. Ti and Ti–7.5Mo substrates were soaked in 20 ml SBF, prepared by dissolving reagent grade NaCl, $NaHCO_3$, KCl, $K_2HPO_4 \cdot 3H_2O$, $MgCl_2 \cdot 6H_2O$, $CaCl_2$ and Na_2SO_4 into distilled water. The final ionic concentrations of the SBF (vs. human plasma) are listed in Table 1 [45]. The treated substrates were immersed in the SBF at 37°C for 1, 7 and 28 days, respectively. The temperature was maintained by using a water bath. After being soaked for selected durations, the specimens were removed from the fluid, washed with distilled water and air-dried. Changes in the c.p. Ti and Ti–7.5Mo surfaces after soaking in SBF were determined by SEM (S-3000 N, Hitachi, Japan). The surface chemical analysis was implemented by energy-dispersive X-ray spectroscopy (EDS) in the SEM. After 28 days, the structural changes occurring on the surfaces due to the aforementioned procedures were investigated by X-ray diffractometry (D8 SSS, Bruker, Germany). To evaluate the ability and rate of apatite formation on the sample surface, changes in the pH values of the SBF at different time intervals were determined by using an electrolyte-type pH meter (Ion 6 meter, Oakton, USA). After each measurement, the SBF was refreshed.

3 Results and discussion

3.1 Surface morphology of samples before and after treatment

Figure 1 shows the surfaces of untreated, NaOH-treated and subsequently Bioglass®-coated c.p. Ti and Ti–7.5Mo, respectively. The surfaces of untreated c.p. Ti and Ti–7.5Mo appeared flat with several grinding marks (Fig. 1a, b). After immersion in 15 M NaOH at 60°C for 24 h, the surfaces of both the c.p. Ti and Ti–7.5Mo substrates exhibited porous network structures, as shown in Fig. 1c and d. A sodium titanate ($Na_2Ti_5O_{11}$) peak appeared between 29° and 30° in 2θ on all XRD patterns (figure not shown) after NaOH treatment of the c.p. Ti and Ti–7.5Mo surfaces, being in agreement with the results reported by Kim et al. [46]. The porous network structures of the sodium titanate layers on the NaOH-treated Ti–7.5Mo were thicker than those on the c.p. Ti. Since the shapes of the pores in the gel layer were thicker and deeper, the shrinkage cracks were visible after drying, in agreement with the results obtained by Rakngarm et al. [47]. After Bioglass® coating, the microporous network structure disappeared, and glass deposits were formed homogeneously on the surfaces of the c.p. Ti (Fig. 1e) and the Ti–7.5Mo (Fig. 1f).

Figure 2 shows the EDS spectra of the surfaces of untreated, NaOH-treated and subsequently Bioglass®-coated c.p. Ti and Ti–7.5Mo, respectively. The EDS analysis of the porous network of NaOH-treated samples revealed the presence of Na, Ti, and O for c.p. Ti and Na, Ti, Mo and O for Ti–7.5Mo (Fig. 2c, d), thereby indicating the existence of a hydrogel phase consisting of $Na_2Ti_5O_{11}$ and TiO_2. The EDS spectra of the Bioglass®-coated samples showed the presence of not only Ti for c.p. Ti (Fig. 2e) and Ti, Mo for Ti–7.5Mo (Fig. 2f), but also Na, Ca, Si, P and O on both metallic surfaces. The minor peaks due to Na, Ca, Si, P and O indicated that the coating was composed of 45S5 Bioglass®.

3.2 Ca–P precipitation on treated surfaces

Figure 3 shows the SEM micrographs of the surface morphology of the c.p. Ti and Ti–7.5Mo specimens after different periods of soaking in SBF. In the present experiments, apatite began to be deposited within 1 day after these immersions and completely covered the entire surfaces of the substrates within 28 days. After 1 day in the SBF, some isolated or aggregated spheroids were deposited on the surfaces of the Ti–7.5Mo; however, only a few tiny particles having a diameter of less than 1 μm were found on the surfaces of the c.p. Ti. After 7 days' immersion in SBF, more aggregated particles were sparsely deposited on the surfaces of both the c.p. Ti and the Ti–7.5Mo. It is noteworthy that much more aggregated spheroids were deposited on the surfaces of the Ti–7.5Mo. Figure 3e and f show that dense and continuous coatings covered all specimens soaked in SBF for 28 days. Moreover, the boundaries of their connections became unclear. The formation of Ca–P layers with a similar morphology has been

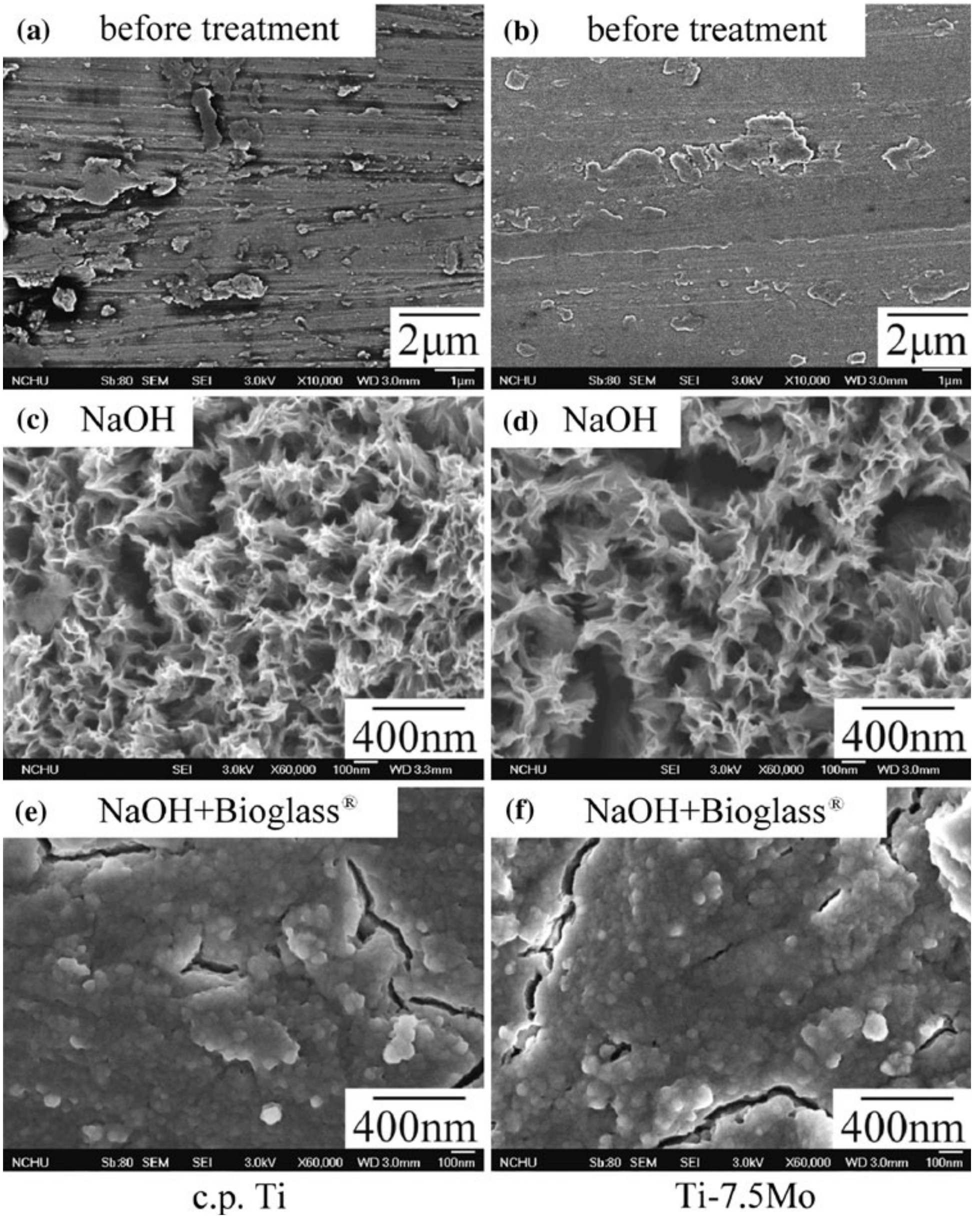

Fig. 1 SEM micrographs of surface morphology of untreated, NaOH-treated and subsequently Bioglass®-coated c.p. Ti (*left*) and Ti–7.5Mo (*right*)

reported for titanium and several of its alloys [40–42]. The cracks in the calcium phosphate layers on both the c.p. Ti and the Ti–7.5Mo probably formed as a result of contractions in the porous hydrated layers when the specimens were dried after being soaked in SBF.

The results of the EDS analysis of the 45S5 Bioglass®-coated c.p. Ti and Ti–7.5Mo surfaces after being soaked in SBF for 28 days, are shown in Fig. 4. After this soaking period, all the specimens exhibited very intensive peaks of Ca and P. The intensities of these peaks were greater in the Ti–7.5Mo specimens than in the c.p. Ti. Moreover, after the same period, no peaks of Ti were detected in the Ti–7.5Mo and c.p. Ti specimens. The intensity of the substrate Ti dramatically decreased due to interference from the calcium phosphate deposits after being soaked, thereby indicating that the coatings were thick enough to prevent the penetration of X-ray beams to the substrate surface. In addition, the lack of Na and Si peaks could be due to the degradation of the 45S5 Bioglass® coatings with the further increase in the calcium phosphate precipitations.

The X-ray diffraction patterns of NaOH-treated and Bioglass®-coated c.p. Ti and Ti–7.5Mo samples, after being soaked in SBF for 28 days, are illustrated in Fig. 5. The distinctive peaks at 26 and 32° (2θ) are evidence that a crystalline HA has formed on the surfaces of each metallic sample. It is noteworthy that peaks of HA appear on both patterns, but the intensities of the peaks are greater for the Ti–7.5Mo specimens. Moreover, after this soaking period, the intensity of the c.p. Ti and Ti–7.5Mo substrates dramatically decreased due to interference from calcium

Fig. 2 EDS of untreated, NaOH-treated and subsequently Bioglass®-coated c.p. Ti (*left*) and Ti–7.5Mo (*right*)

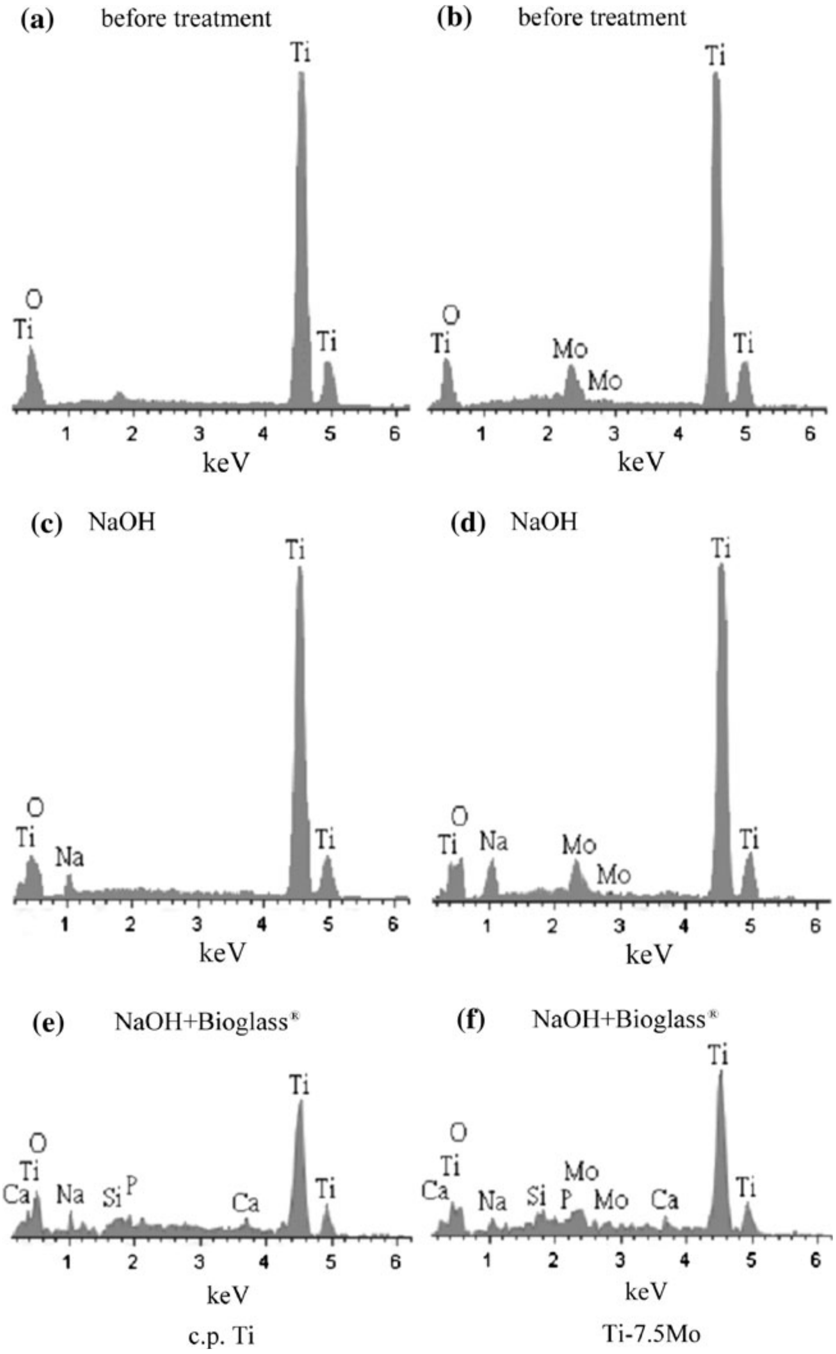

phosphate deposits. It can be concluded that the calcium phosphate deposits are greater for NaOH-treated and Bioglass®-coated Ti–7.5Mo than for c.p. Ti, a conclusion in agreement with the EDS results depicted in Fig. 4.

In our previous study [48], the apatite did not start to deposit until the third day after immersion of only the NaOH-treated samples. However, when a combination of NaOH treatment and subsequent Bioglass® coating was used, the apatite began to deposit within one day after immersion in the SBF. Consequently, c.p. Ti and Ti–7.5Mo subjected to NaOH treatment and subsequent Bioglass® coating show a greater level of high apatite-forming ability than that of c.p. Ti and Ti–7.5Mo subjected to only NaOH treatments.

The pH value of the SBF after the incubation process was found to increase gradually during the immersion of the NaOH-treated and Bioglass®-coated metallic samples, thus indicating an increasing concentration of hydroxyl group (OH^-) ions. This pH approached peaks of 7.66 for the Ti–7.5Mo and 7.61 for the c.p. Ti on the first day after

Fig. 3 SEM micrographs of surface morphology of NaOH-treated and subsequently Bioglass®-coated c.p. Ti (*left*) and Ti–7.5Mo (*right*) after various soaking periods in SBF

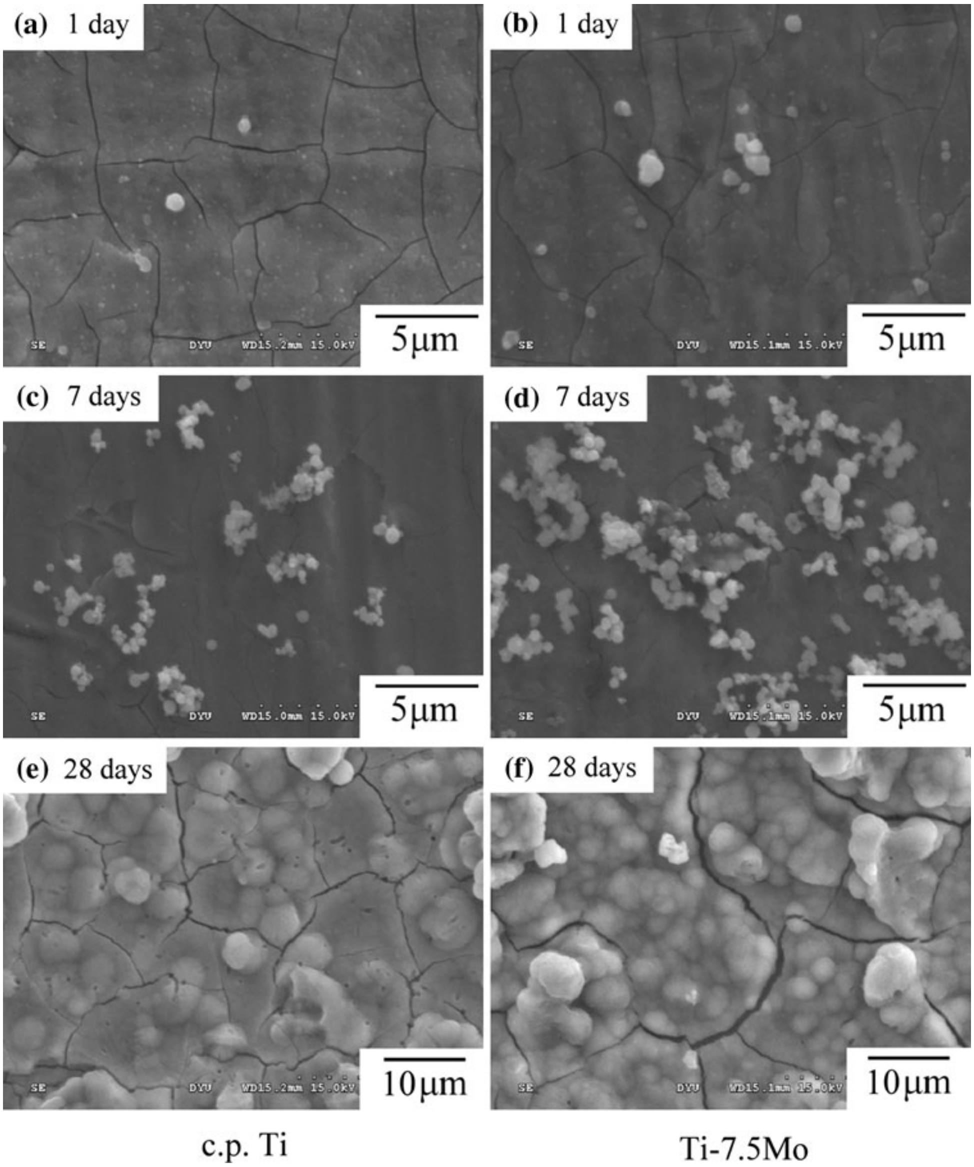

the NaOH treatment and the Bioglass®-coating. However, the pH approached peaks of 7.61 for the NaOH-treated Ti–7.5Mo and 7.57 for the NaOH-treated c.p. Ti on the third day, as graphed in Fig. 6. It was proposed that the pH increase resulted from the dissolution of Na^+ ions out of the titanate gel in exchange with H^+ ions in SBF and that this was considered important for apatite deposition [46]. The released Na^+ ions increase the degree of supersaturation of the soaking solution with respect to apatite by increasing pH, and the titanium oxide hydrogel induces apatite nucleation on the titanium surface [49]. It can be supposed that the higher the amount of Na^+ released, the higher pH and the higher supersaturation. Therefore, the higher pH value and apatite-forming ability of the surface-treated Ti–7.5Mo may be attributed to the greater amount of Na^+ ions in the surface gel layer, which is composed of sodium titanate and Bioglass® coating.

Bioglass® releases Na^+ ions into a SBF via an exchange with the H_3O^+ ions in the fluid to form Si–OH groups on the surface [50, 51]. An increasing number of Na^+ ions released into this SBF finally increased the pH in the vicinity of the surface. These Si–OH groups formed immediately combined with Ca^{2+} ions in the fluid to form an amorphous calcium silicate on the glass surface. After a long soaking period, this calcium silicate characteristically combines with phosphate ions in the fluid to form an amorphous calcium phosphate and this phase later transforms into bone-like apatite crystals [52]. The apatite formation from the constituent ions is given by the following equation [18]:

$$10Ca^{2+} + 6PO_4^{3-} + 2OH^- \rightarrow Ca_{10}(PO_4)_6(OH)_2$$

The apatite nuclei were initiated once the supersaturation rose above the critical level necessary for heterogeneous

Fig. 4 EDS of NaOH-treated and subsequently Bioglass®-coated c.p. Ti and Ti–7.5Mo after soaking in SBF for 28 days

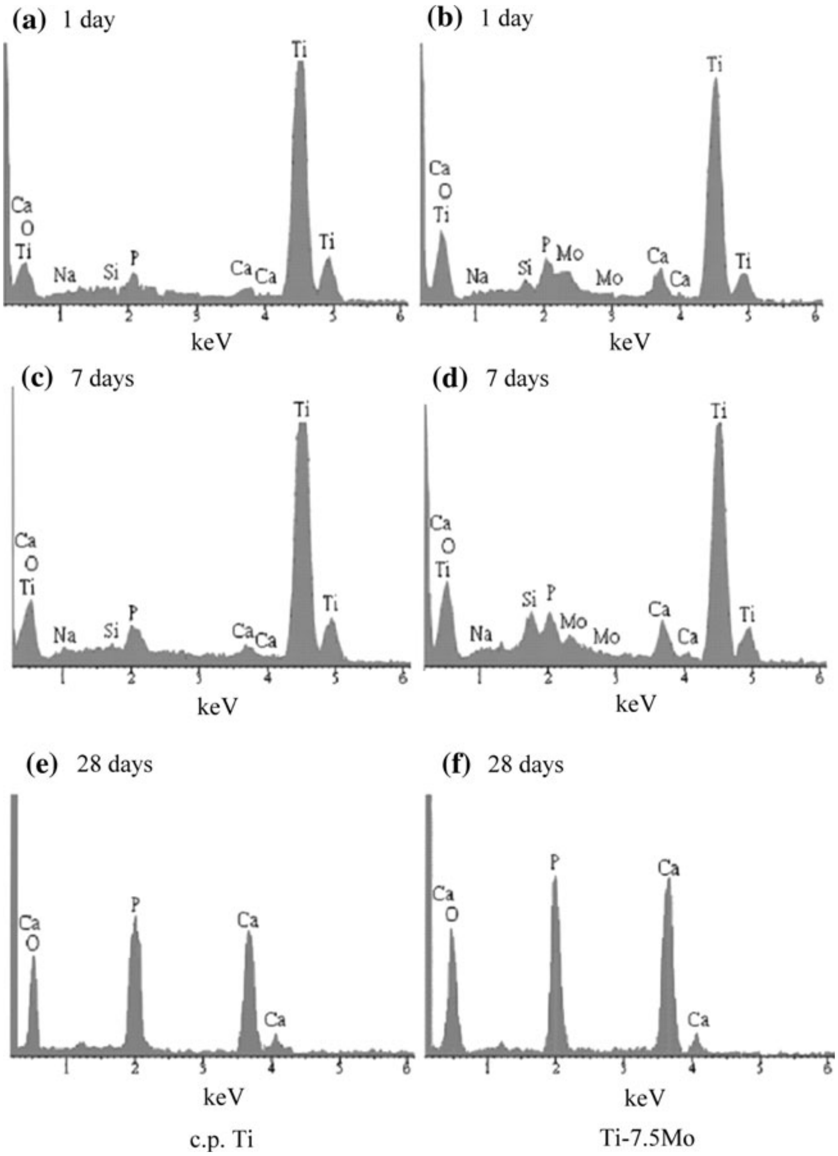

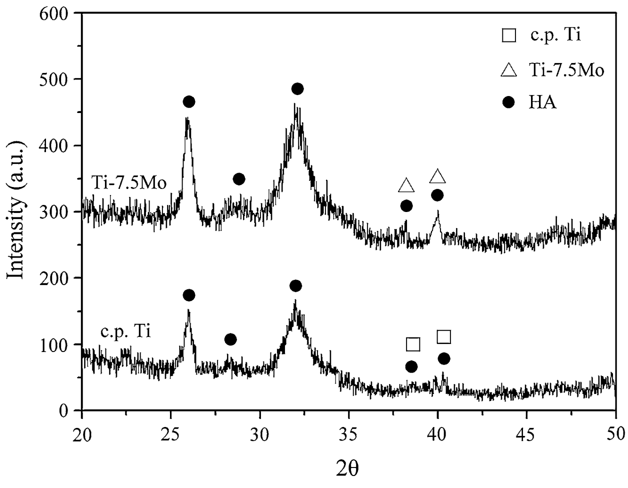

Fig. 5 XRD patterns of NaOH-treated and subsequently Bioglass®-coated c.p. Ti and Ti–7.5Mo after soaking in SBF for 28 days

nucleation of apatite. The observed pH increase during the immersion of the surface-treated c.p. Ti and Ti–7.5Mo in the SBF (as shown in Fig. 6) is in agreement with previous studies of alkali- and heat-treated Ti and its alloys [46, 53]. Once the apatite nuclei were formed, they could spontaneously grow by consuming the calcium, phosphate and OH^- ions from the SBF. After the consumption of the OH^- ions, the pH of the fluid should decrease as the apatite begins to deposit [54]. In the present experiments, the apatite began to deposit within 1 day after immersion of the NaOH-treated and Bioglass®-coated samples in the SBF, thus corresponding very well with the peak pH value on the first day. Moreover, in our previous study [48], the apatite began to deposit within 3 days after immersion of the NaOH-treated samples, thereby corresponding favorably with the peak pH value on that day. However, the calcium phosphate deposits were greater for the

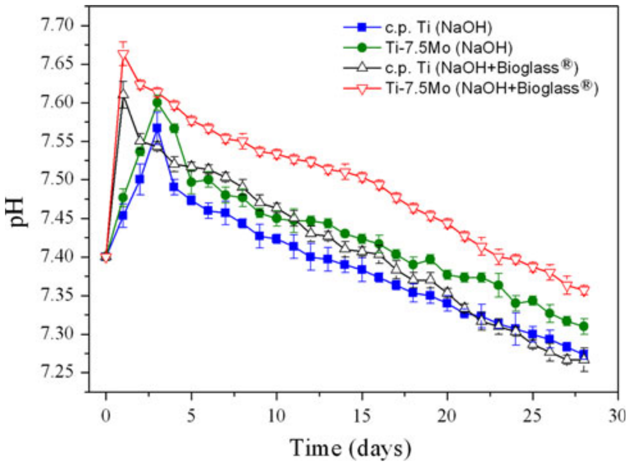

Fig. 6 pH value of SBF as a function of soaking time for c.p. Ti and Ti–7.5Mo subjected to NaOH treatment or NaOH treatment and subsequently Bioglass® coating

NaOH-treated and Bioglass®-coated Ti–7.5Mo than for the c.p. Ti, as indicated in the results from EDS (Fig. 4) and XRD (Fig. 5). Furthermore, the deposited amounts of calcium phosphate were also much greater for alkali-treated Ti–7.5Mo than for alkali-treated c.p. Ti, as evaluated in the previous study [48]. These results could be correlated with the higher pH value of the SBF containing surface-treated Ti–7.5Mo.

Bioglass® can be an attractive candidate for surface modification of implanted devices, since it is an approved bioactive material having preexisting long-term safety data. Possible applications could entail the post-modification of pre-packaged or custom-made titanium-based implants. Finally, Bioglass® has been demonstrated to be active against supra- and sub-gingival bacteria [55], thus further emphasizing its potential benefits when in contact with an implanted device.

4 Conclusions

(1) The surfaces of both NaOH-treated c.p. Ti and Ti–7.5Mo substrates exhibited microporous network structures. After Bioglass® coating, the microporous network structure disappeared and glass deposits were formed homogeneously on the surfaces of both substrates.

(2) The apatite began to deposit within 1 day after immersion of the c.p. Ti and the Ti–7.5Mo in SBF and completely covered the entire surfaces of the substrates within 28 days. Moreover, more aggregated spheroids were deposited on the surfaces of the Ti–7.5Mo after immersion for 1 and 7 days, respectively.

(3) On the basis of the results from EDS analysis after soaking in SBF for 28 days, all the c.p. Ti and Ti–7.5Mo specimens exhibited very intensive peaks of Ca and P. Moreover, the intensity of both substrates dramatically decreased due to interference from calcium phosphate deposits. The results from both EDS and XRD indicated that the calcium phosphate deposits were greater for the NaOH-treated and Bioglass®-coated Ti–7.5Mo than for the c.p. Ti.

(4) The pH value of the SBF approached peaks of 7.66 for the Ti–7.5Mo and 7.61 for the c.p. Ti on the first day after the NaOH treatment and the Bioglass®-coating. However, the pH approached peaks of 7.61 for the NaOH-treated Ti–7.5Mo and 7.57 for the NaOH-treated c.p. Ti on the third day. Moreover, the calcium phosphate deposits were greater for the NaOH-treated and Bioglass®-coated Ti–7.5Mo than for the c.p. Ti, which could be correlated with the higher pH value of the SBF containing surface-treated Ti–7.5Mo.

Acknowledgement The authors express appreciation to Dr. Cheryl Rutledge, Associate Professor of English, Da-Yeh University, for her editorial assistance.

References

1. Sennerby L, Thomson P, Ericsen LE. Immobilization of type I collagen on the alloy Ti6A14V. J Mater Sci Mater Med. 1992;3:262–71.
2. Takatsuka K, Yamamuro T, Nakamura T, Kokubo T. Bone-bonding behavior of titanium alloy evaluated mechanically with detaching failure load. J Biomed Mater Res. 1995;29:157–63.
3. Yan WQ, Davies JE. Bone formation around surface modified titanium implants bioceramics. Bioceramics. 1998;11:659–62.
4. Nishiguchi S, Nakamura T, Kobayashi M, Kim HM, Miyaji F, Kokubo T. The effect of heat treatment on bone-bonding ability of alkali-treated titanium. Biomaterials. 1999;20:491–500.
5. Morris HF, Ochi S, Spray JR, Olson JW. Periodontal-type measurements associated with hydroxyapatite-coated and non-HA-coated implants: uncovering to 36 months. Ann Periodontol. 2000;5:56–67.
6. Geurs NC, Jeffcoat RL, McGlumphy EA, Reddy MS, Jeffcoat MK. Influence of implant geometry and surface characteristics on progressive osseointegration. Int J Oral Maxillofac Implants. 2002;17:811–5.
7. Barrère F, van der Valk CM, Meijer G, Dalmeijer RAJ, de Groot K, Layrolle P. Osteointegration of biomimetic apatite coating applied onto dense and porous metal implants in femurs of goats. J Biomed Mater Res. 2003;67B:655–65.
8. Ong JL, Lucas LC, Lacefield WR, Rigney ED. Structure, solubility and bond strength of thin calcium phosphate coatings produced by ion beam sputter deposition. Biomaterials. 1992;13:249–54.
9. Ducheyne P, Radin S, Heughebaert M, Heughebaert JC. Calcium phosphate coatings on metallic porous surfaces. Biomaterials. 1990;11:244–54.
10. Albayrak O, El-Atwani O, Altintas S. Hydroxyapatite coating on titanium substrate by electrophoretic deposition method: Effects

of titanium dioxide inner layer on adhesion strength and hydroxyapatite decomposition. Surf Coat Technol. 2008;202: 2482–7.

11. Boyd AR, Duffy H, McCann R, Meenan BJ. Sputter deposition of calcium phosphate/titanium dioxide hybrid thin films. Mater Sci Eng C. 2008;28:228–36.
12. Im KH, Lee SB, Kim KM, Lee YK. Improvement of bonding strength to titanium surface by sol–gel derived hybrid coating of hydroxyapatite and titania by sol–gel process. Surf Coat Technol. 2007;202:1135–8.
13. de Groot K, Geesink RGT, Klein CPAT, Serekian P. Plasma sprayed coatings of hydroxylapatite. J Biomed Mater Res. 1987;21:1375–81.
14. Klein CAPT, Patka P, van der Lubbe HBM, Wolke JGC, de Groot K. Plasma sprayed coating of tetracalcium phosphate, hydroxyapatite, and a-KNIGHT on titanium alloy: an interfacial study. J Biomed Mater Res. 1991;25:53–65.
15. Radin SR, Ducheyne P. Calcium phosphate ceramic coatings as carriers of vancomycin. J Mater Sci Mater Med. 1992;3:33–42.
16. Han Y, Fu T, Lu J, Xu K. Characterization and stability of hydroxyapatite coatings prepared by an electrodeposition and alkaline-treatment process. J Biomed Mater Res. 2001;54: 96–101.
17. Li P, Ohtsuki C, Kokubo T, Nakanishi K, Soga N, de Groot K. The role of hydrated silica, titania and alumina in inducing apatite on implants. J Biomed Mater Res. 1994;28:7–15.
18. Li P, Kangasniemi I, de Groot K, Kokubo T. Bonelike hydroxyapatite induction by a gel-derived titania on a titanium substrate. J Am Ceram Soc. 1994;5:1307–12.
19. Ohtsuki C, Iida H, Hayakawa S, Osaka A. Bioactivity of titanium treated with hydrogen peroxide solution containing metal chlorides. J Biomed Mater Res. 1997;35:39–47.
20. Wang XX, Hayakawa S, Tsuru K, Osaka A. A comparative study of in vitro apatite deposition on heat-, H_2O_2-, and NaOH-treated titanium surfaces. J Biomed Mater Res. 2001;54:172–8.
21. Kokubo T, Kushitani H, Sakka S, Kitsugi T, Yamamuro T. Solutions able to reproduce in vivo surface-structure changes in bioactive glass-ceramic A-W3. J Biomed Mater Res. 1990;24: 721–34.
22. Kokubo T, Takadama H. How useful is SBF in vivo bone bioactivity? Biomaterials. 2006;27:2907–15.
23. Habibovic P, Li J, van der Valk CM, Meijer G, Layrolle P, van Blitterswijk CA, et al. Biological performance of uncoated and octacalcium phosphate-coated Ti6Al4V. Biomaterials. 2005;26: 23–36.
24. Bil M, Ryszkowska J, Roether JA, Bretcanu O, Boccaccini AR. Bioactivity of polyurethane-based scaffolds coated with Bioglass®. Biomed Mater. 2007;2:93–101.
25. Roether JA, Boccaccini AR, Hench LL, Maquet V, Gautier S, Jérôme R. Development and in vitro characterisation of novel bioresorbable and bioactive composite materials based on polylactide foams and Bioglass® for tissue engineering applications. Biomaterials. 2002;23:3871–8.
26. Bretcanu O, Verné E, Borello L, Boccaccini AR. Bioactivity of degradable polymer sutures coated with bioactive glass. J Mater Sci Mater Med. 2004;15:893–9.
27. Trentani L, Pelillo F, Pavesi FC, Ceciliani L, Cetta G, Forlino A. Evaluation of the $TiMo_{12}Zr_6Fe_2$ alloy for orthopaedic implants: in vitro biocompatibility study by using primary human fibroblasts and osteoblasts. Biomaterials. 2002;23:2863–9.
28. Lin DJ, Chern Lin JH, Ju CP. Structure and properties of Ti–7.5Mo–xFe alloys. Biomaterials. 2002;23:1723–30.
29. Ho WF, Chiang TY, Wu SC, Hsu HC. Mechanical properties and deformation behavior of cast binary Ti–Cr alloys. J Alloys Compd. 2009;468:533–8.
30. Okazaki Y, Nishimura E. Effect of metal released from Ti alloy wear powder on cell viability. Mater Trans. 2000;41:1247–55.
31. Okazaki Y, Rao S, Ito Y, Tateishi T. Corrosion resistance, mechanical properties, corrosion fatigue strength and cytocompatibility of new Ti alloys without Al and V. Biomaterials. 1998;19:1197–215.
32. Oliveira NTC, Ferreira EA, Duarte LT, Biaggio SR, Rocha-Filho RC, Bocchi N. Corrosion resistance of anodic oxides on the Ti–50Zr and Ti–13Nb–13Zr alloys. Electrochim Acta. 2006;51: 2068–75.
33. Hao YL, Li SJ, Sun SY, Zheng CY, Yang R. Elastic deformation behavior of Ti–24Nb–4Zr–7.9Sn for biomedical applications. Acta Biomater. 2007;3:277–86.
34. Pipino F. The bone-prosthesis interaction. J Orthop Traumatol. 2000;1:3–9.
35. Ho WF, Ju CP, Chern LJH. Structure and properties of cast binary Ti–Mo alloys. Biomaterials. 1999;20:2115–22.
36. Ho WF. A comparison of tensile properties and corrosion behavior of cast Ti–7.5Mo with c.p. Ti, Ti–15Mo and Ti–6Al–4V alloys. J Alloys Compd. 2008;464:580–3.
37. Habibovic P, Barrère F, van Blitterswijk CA, de Groot K, Layrolle P. Biomimetic hydroxyapatite coating on metal implants. J Am Ceram Soc. 2002;85:517–22.
38. Ma J, Wong H, Kong LB, Peng KW. Biomimetic processing of nanocrystallite bioactive apatite coating on titanium. Nanotechnology. 2003;14:619–23.
39. Barrère F, Snel MME, van Blitterswijk CA, de Groot K, Layrolle P. Nano-scale study of the nucleation and growth of calcium phosphate coating on titanium implants. Biomaterials. 2004;25: 2901–10.
40. Jonášová L, Müller FA, Helebrant A, Strnad J, Greil P. Biomimetic apatite formation on chemically treated titanium. Biomaterials. 2004;25:1187–94.
41. Faure J, Balamurugan A, Benhayoune H, Torres P, Balossier G, Ferreira JMF. Morphological and chemical characterisation of biomimetic bone like apatite formation on alkali treated Ti6Al4V titanium alloy. Mater Sci Eng C 2008; doi:10.1016/j.msec.2008.09.047.
42. Kokubo T. Bioactive glass ceramics: properties and applications. Biomaterials. 1991;12:155–63.
43. Hench LL. Bioceramics: from concept to clinic. J Am Ceram Soc. 1991;74:1487–510.
44. Kokubo T, Kim HM, Kawashita M, Nakamura T. Bioactive metals: preparation and properties. J Mater Sci Mater Med. 2004;15:99–107.
45. Li P, Ohtsuki C, Kokubo T, Nakanishi K, Soga N, Nakamura N, et al. The role of hydrated silica, titania, and alumina in inducing apatite on implants. J Mater Sci Mater Med. 1993;4:127–31.
46. Kim HM, Miyaji F, Kokubo T, Nakamura T. Preparation of bioactive Ti and its alloys via simple chemical surface treatment. J Biomed Mater Res. 1996;32:409–17.
47. Rakngarm A, Miyashita Y, Mutoh Y. Formation of hydroxyapatite layer on bioactive Ti and Ti–6Al–4V by simple chemical technique. J Mater Sci Mater Med. 2008;19:1953–61.
48. Ho WF, Lai CH, Hsu HC, Wu SC. Surface modification of a low-modulus Ti–7.5Mo alloy treated with aqueous NaOH. Surf Coat Technol. 2009;203:3142–50.
49. Kokubo T, Miyaji F, Kim HM. Spontaneous formation of bonelike apatite layer on chemically treated titanium metals. J Am Ceram Soc. 1996;79:1127–9.
50. Takadama H, Kim HM, Kokubo T, Nakamura T. Mechanism of biomineralization of apatite on a sodium silicate glass: TEM-EDX study in vitro. Chem Mater. 2001;13:1108–13.
51. Takadama H, Kim HM, Kokubo T, Nakamura T. X-ray photoelectron spectroscopy study on the process of apatite formation

on a sodium silicate glass in simulated body fluid. J Am Ceram Soc. 2002;85:1933–6.

52. Kokubo T, Kim HM, Kawashita M. Novel bioactive materials with different mechanical properties. Biomaterials. 2003;24: 2161–75.
53. Kim HM, Takadama H, Miyaji F, Kokubo T, Nishiguchi S, Nakamura T. Formation of bioactive functionally graded structure on Ti–6Al–4V alloy by chemical surface treatment. J Mater Sci Mater Med. 2000;11:555–9.
54. Chen X, Nouri A, Li Y, Lin J, Hodgson PD, Wen C. Effect of surface roughness of Ti, Zr, and TiZr on apatite precipitation from simulated body fluid. Biotechnol Bioeng. 2008;1:378–87.
55. Allan I, Newman H, Wilson M. Antibacterial activity of particulate Bioglass® against supra-and subgingival bacteria. Biomaterials. 2001;22:1683–7.